Scanning Electron Microscope Studies on the Breakdown of Passivity of a Nickel-Chromium-Molybdenum Dental Alloy

J. Geis-Gerstorfer
School of Dentistry

W. Göpel
University of Tübingen

H. Weber
School of Dentistry

Utah State University
MERRILL-CAZIER LIBRARY

SCANNING ELECTRON MICROSCOPE STUDIES ON THE BREAKDOWN OF
PASSIVITY OF A NICKEL-CHROMIUM-MOLYBDENUM DENTAL ALLOY.

J. Geis-Gerstorfer [1*] , W. Göpel[2] , H. Weber [1]

1   Department of Prosthetics II
School of Dentistry
Osianderstrasse 2-8
2   Institute of Physical and Theoretical Chemistry
Auf der Morgenstelle 8
University of Tübingen
D-7400 Tübingen
West Germany

Abstract

The breakdown of passivity and localized corrosion of a Ni-20Cr-10Mo alloy was investigated. The methods employed were potentiodynamic polarization and SEM, and AES and EDX after potentiostatic polarization over a period of 20 hours in the passive and transpassive regions. The 1 μm finished as-cast specimens were polarized in aerated 0.1 M NaCl. The cyclic polarization curves revealed a critical pitting potential of 470 mV (SCE), while the protection potential was 300 mV (SCE). Using the potentiostatic polarization technique, nearly constant corrosion currents appeared, indicating that the whole surface was corroded uniformly. SEM pictures of samples, corroded at 650 mV, showed little pits under the oxide layer and a thinning down of the outer oxide layer. This lead to the opinion that the penetration as well as the adsorption mechanism determine the breakdown of passivity. EDX analysis and AES depth profiles showed an enrichment of Cr and Mo in the oxide. In contrast to oxidized samples, no second layer of Ni was found in the outer oxide region. In the transpassive region the relative amount of Cr and Mo in the oxide layer was higher than the one found in corresponding samples polarized in the passive region. The oxide thickness found was about 5 nm in the passive region (300 mV SCE) and about 250 nm in the transpassive region (650 mV SCE).

* Address for correspondence:
School of Dentistry
Osianderstrasse 2-8
D-7400 Tübingen
W. Germany   Phone No. 07071-295152

Introduction

The continued fluctuations in the price of precious alloys lead to the development of dental alloys made of less expensive constituents. The components of non-precious alloys mainly available are nickel (60 to 80 wt.%), chromium (12 to 24 wt.%) and molybdenum (0 to 14 wt.%). Both, electrochemical measurements [6] and substance loss measurements [7] showed a broad spectrum of corrosion resistance of Ni-Cr-Mo alloys depending on their chemical composition.

An effective passive film must keep the corrosion on an alloy surface quite low because small amounts of corrosion products can cause local tissue reactions [2,5]. In order to remain effective, the passive layer must resist the breakdown processes of aggressive anions in the saliva. The chemical breakdown is poorly understood. A description of the various modes has been summarized by Evans [4] and Strehblow [12]. The main mechanisms discussed in the literature are the penetration mechanism [8], the adsorption mechanism [9] and the film breaking mechanism [10,11]. The penetration mechanism involves the migration of aggressive anions through the oxide to the metal oxide interface causing pit nucleation. The adsorption mechanism is based on a local adsorption of the aggressive anions at the surface of the passivating oxide leading to an increased dissolution of the oxide. The film breaking mechanism postulates a mechanical breakdown of the oxide layer with direct access of the anions to the metal surface. But the film breaking mechanism seems to play a minor role under stationary conditions [12]. All these mechanisms involve damaging species. One of the major species causing breakdown of passivity is the chloride ion, abundantly available in saliva with an average of 600 to 700 mg/l chlorine. Another important specie is thiocyanate, whose influence has been described elsewhere [7].

This in vitro investigation has been carried out in order to study the breakdown of passivity and localized corrosion of an Ni-20Cr-10Mo alloy and is part of a program investigating the influence of different molybdenum contents on the corrosion behaviour.

Materials and Methods

An experimental Ni-20Cr-10Mo alloy was prepared from high-purity nickel (99.996 wt.%), chromium (99.999 wt.%) and molybdenum (99.95 wt.%) in order to avoid corrosion effects of minor constituents. After arc melting in argon the alloy was melted in a dental induction casting machine (Nautilus, BEGO, FRG). The samples, $10 \times 5 \times 1$ mm^3 thick, were prepared by polishing the specimens to a 1 μm finish, using diamond paste and were then ultrasonically cleaned in methanol.

Cyclic potentiodynamic polarization curves sweeping to a threshold current of 1×10^{-3} A/cm^2 with a scan rate of 0.005 mV/s starting at -250 mV versus E_{corr} (SCE) and potentiostatic polarization curves over a period of 20 h (100 measurements/h), were taken in the passive and transpassive region to characterize the corrosion behaviour. A

Fig. 1: Schematic representation of the corrosion cell: A = working electrode (Pt-wire), B = reference electrode, C = counter electrode.

commercial computer controlled potentiostat (Model 351, EG&G Princeton Applied Research,USA), and a standard corrosion cell (Fig. 1) with a saturated calomel electrode (SCE) were used. The electrolyte employed was aerated 0.1 M sodium chloride solution controlled to a temperature of 37 ±1 °C.

To study the corroded surfaces of the alloy, scanning electron microscopy (Stereoscan 250, CAMBRIDGE,England) was used connected with energy dispersive X-ray (EDX) analysis (Model 9100, EDAX-International, USA). All EDX-spectra were carried out with primary electron energies of 15 keV using a magnification of 10,000 (window technique), and about 3000 CPS for data acquisition. In order to analyse oxygen with EDX a windowless detector was used.

More detailed analysis of chemical distribution of the layers grown in the passive and transpassive region were obtained with a scanning Auger microprobe (Model 610, Perkin-Elmer,USA). Ion milling was done with Argon rastered over an area of 1×1 mm^2 in order to remove layers of oxide. The pressure in the chamber during depth profiling was about 2×10^{-8} mbar. A 5 keV primary electron beam (1000 nA) was used to excite those spectra. Auger spectra were taken to provide a profile of the atomic constituents (Ni, Cr, Mo, O, C) present as a function of depth into the bulk alloy. The sputtering rate was determined with calibrated tantalum oxide for each ion-energy depth profile to obtain the interface width.

Results

The cyclic potential-current density profile of Ni-20Cr-10Mo is shown in Figure 2. The corrosion current in the passive region was about 8×10^{-8} A/cm^2 without any active peak. The transition from passivity to transpassivity was clearly defined. The breakdown of passivity occurred at a critical pitting potential E_c of 470 mV (10^{-7} A/cm^2). After reaching the threshold current of 1×10^{-3} A/cm^2 the scan direction was reversed causing repassivation of the pits. The resulting small hysteresis loop of the potential-current function indicates that Ni-20Cr-10Mo has little tendency to pit. The protection potential against pitting E_p, defined as the point where the reverse scan intersects the forward scan, was 300 mV (SCE).

Potentiostatic polarization measurements were used to obtain more information about the pitting characteristics (Fig. 3). The results revealed nearly constant corrosion currents during the time the potentials were applied. This is of great importance because it points out
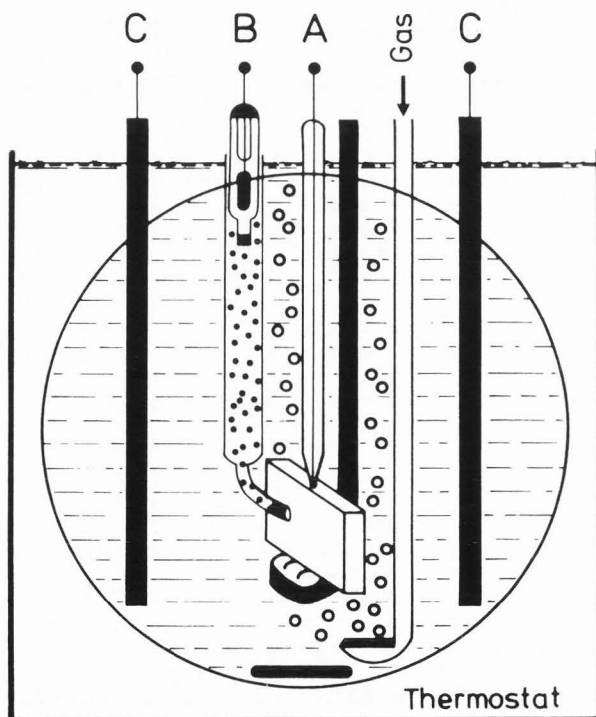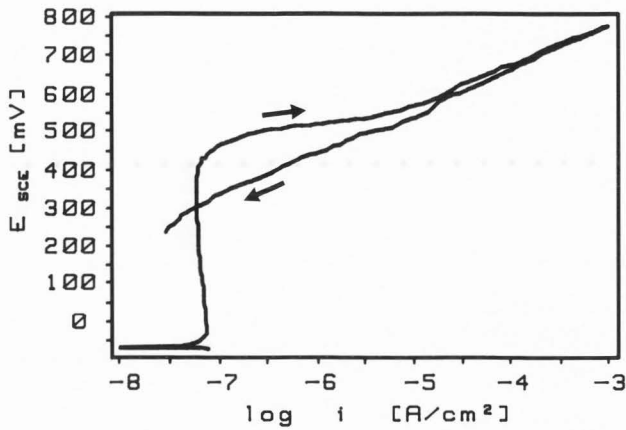
Fig. 2: Potentiodynamic polarization curve of Ni-20Cr-10Mo in aerated 0.1 M NaCl (sweep rate 0.005 mV/s).

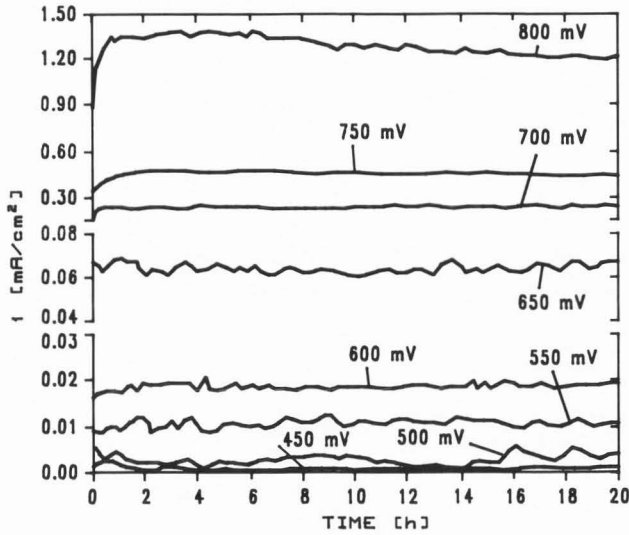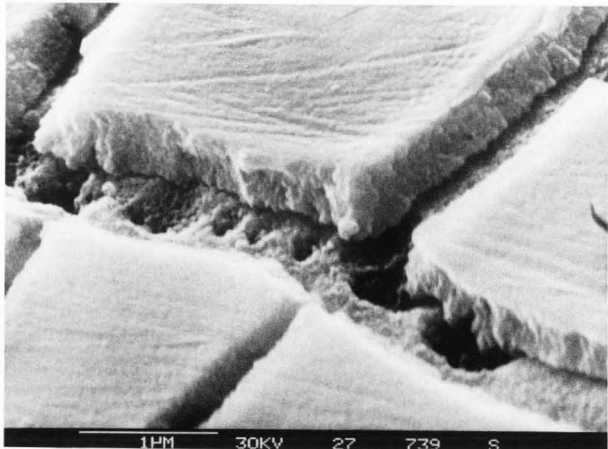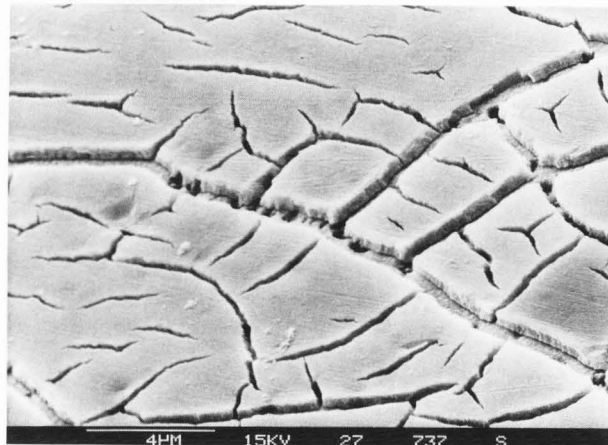**Fig. 3:** Potentiostatic polarization curves of Ni-20Cr-10Mo at various potentials (SCE) in aerated 0.1 M NaCl.

found under the layer. This may involve the penetration of Cl-ions through the passive layer to the metal surface. The SEM images showed that the oxide film increased with the potential. The surface was covered completely with the passive layer and no distinct localized pitting was visible. Even when using higher potentials (e.g., 800 mV), the formation of a passive layer was not prevented. This indicates that the whole surface acts as a corrosion pit with a planar geometry, but the oxide growth is fast enough to build a new layer spontaneously in the potential region to 800 mV.

Many Cr-particles (probably Cr_2O_3) up to 2 μm in diameter could be observed (Fig. 5), which represent the original surface towering above the corroded surface. This indicates that the oxide film is thinned uniformly which is caused by adsorption of aggressive Cl-ions. Intensified corrosion around the Cr-particles (crevice corrosion, contact

that the whole surface is corroded uniformly.

Typical surface topographies of Ni-20Cr-10Mo, after 20 h potentiostatic polarization at 650 mV (SCE), are shown in the SEM images of Figure 4. Many cracks in the surface layer were found, as a result of drying. However, using samples corroded at potentials lower than 500 mV no cracks could be observed due to the better elasticity of the thinner layers. The film thickness on samples polarized at 650 mV in the active region was 200 to 300 nm. Looking into the cracks (Fig. 4) many little pits were

Figs. 4 a,b: SEM micrographs of Ni-20Cr-10Mo after 20 h of polarization at 650 mV (SCE) in aerated 0.1 M NaCl.

Fig. 7: The oxide layer was thinned down at the metal/oxide interface (E=650 mV).
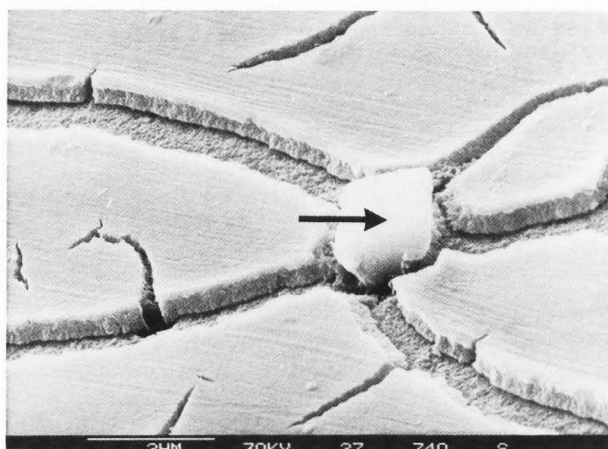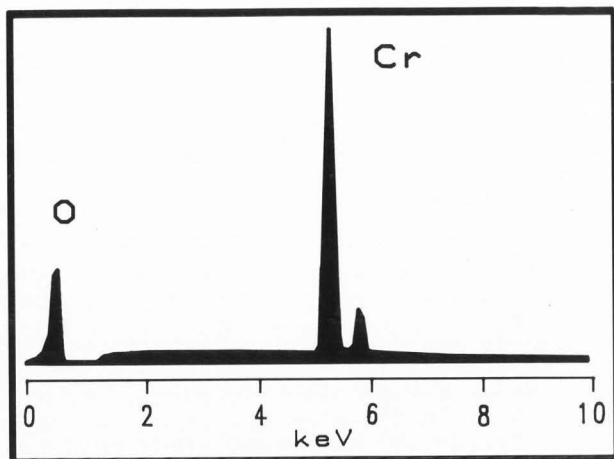

Fig. 5: SEM micrograph of a Cr-particle representing the original surface (E=650 mV) and EDX spectrum.

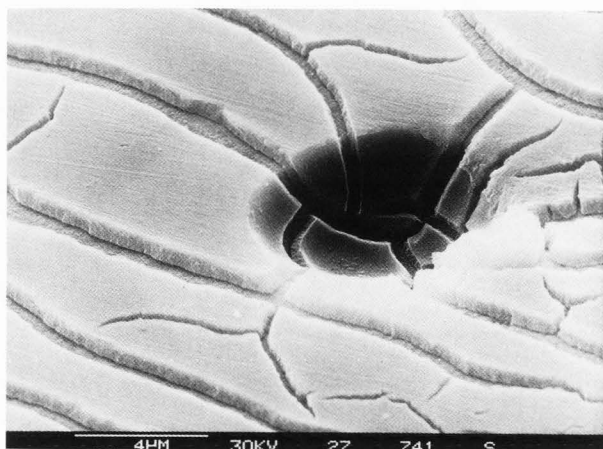Fig. 6: After a removal of Cr-particles the pits were passivated (E=650 mV).
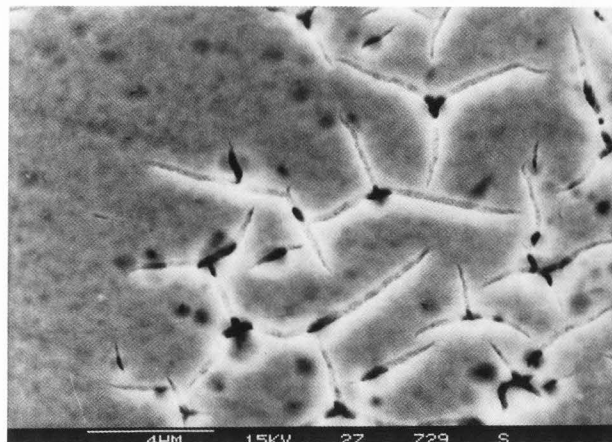
corrosion) lead to a removal of the particles from the sample. However, the pits developed in this way were passivated (Fig. 6). At advanced stages of corrosion attack the oxide layer was thinned down beginning at the metal surface oxide interface, but no local pitting has been found. This effect was visible by dark spots in the layer (Fig. 7) with a maximum of 1 μm in diameter.

A comparison of EDX analysis of the corroded surface potentiostatically polarized at 650 mV, measured with oxide layer and in the cracks without oxide layer (Fig. 4), is shown in figures 8 and 9. An accumulation of chromium, molybdenum and oxygen was found in the passive layer, whereas nickel was the same. However, EDX ought to be used cautiously for the examination of thin oxide layers because the analyzing beam's penetration (0.5-1.0 μm in diameter) into the alloy might lead to errors.

Therefore AES concentration profiles were taken from samples polarized at 300 mV and 650 mV. The survey spectrum of the surface which was to be exposed to the corrosion tests is shown in Figure 10. The depth profile in the passive region and the survey spectra before and after ion-milling are shown in Figures 11 to 16. Unfortunately, it was not possible to clearly differentiate chlorine from molybdenum because of their similar major peaks at 181 eV (Cl) and 186 eV (Mo). In order to circumvent this problem molybdenum was registered at 2044 eV (Fig. 10).

In contrast to results obtained with oxidized samples at high temperatures [1,3], no second layer of nickel was found in the outer oxide with samples not exposed to the corrosion test and samples polarized at 300 mV; probably as a result of dissolving processes. After a signifi-
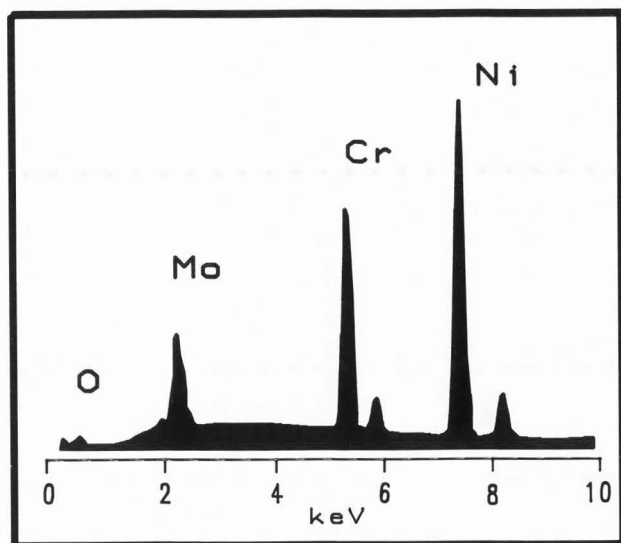
Fig. 8 : EDX spectra of the corroded surface measured without the protective oxide layer (E=650 mV SCE).
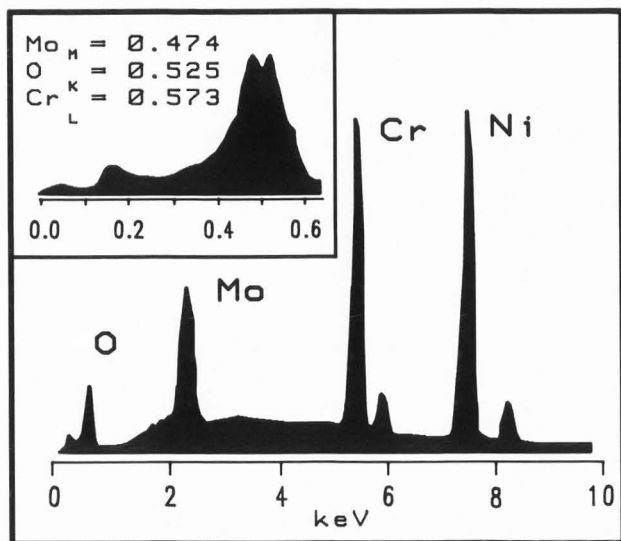

Fig. 9 : EDX spectra of the corroded surface measured with the protective oxide layer (E=650 mV SCE).

cant drop in carbon contamination and oxygen content has occurred, a Cr-rich oxide was detected followed by a Cr-depletion (Fig. 14). Molybdenum was distributed throughout the oxide uniformly, with the exception of little enrichment after having sputtered 6-7 minutes. The oxide thickness was about 5 nm compared with calibrated tantalum oxide. After 10 minutes of sputtering the sputter rate was raised to a factor of 100 until the bulk concentration appeared. The depth
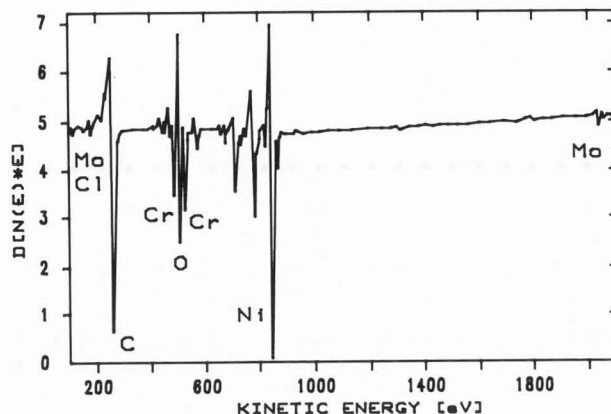

Fig. 10: AES spectrum of the surface which was to be exposed to the corrosion tests.

profile showed that nickel was enriched in the inner oxide.

The nickel and chromium distributions in the oxides on samples polarized at 650 mV in the transpassive region were somewhat different from those encountered previously. The relative amount of chromium and molybdenum in the oxide layer was higher (Fig. 15) than those amounts found in corresponding samples polarized at 300 mV in the passive region. This is in accordance with the results of EDX analysis. The oxide layer was scaled up 50 times to a thickness of 250 nm. Chromium was the predominant element in the outer oxide and had a nearly constant level throughout the layer just as molybdenum. Nickel increased slightly until a drop in the oxygen content occurred and raised then to the bulk level. The AES survey spectra before and after ion-milling are shown in Figs. 14 and 16.

Summary

Several general conclusions can be drawn regarding the mechanism for breakdown of the passive film and the element distribution in oxides formed at corroded Ni-20Cr-10Mo. The results of SEM studies indicate that the penetration mechanism as well as the adsorption mechanism determine the overall reaction. The passivation potential and the potential for transpassive dissolution is determined by the chromium and molybdenum concentration, both of which are enriched in the outermost surface layer. In contrast to alloys containing less molybdenum, no distinct localized pitting occurred. The alloy was dissolved uniformly starting at a potential of 470 mV (SCE). The protection current against pitting was 300 mV (SCE). The oxide layer produced in the
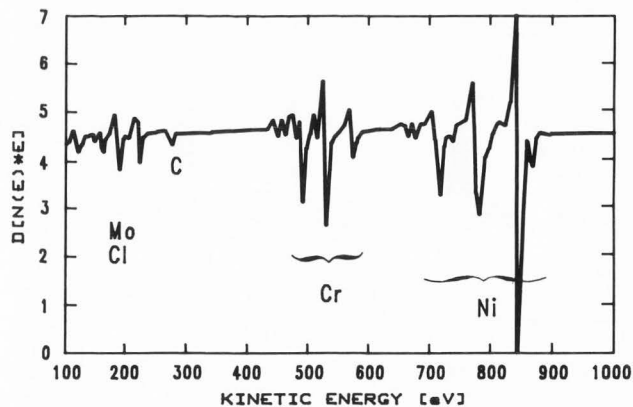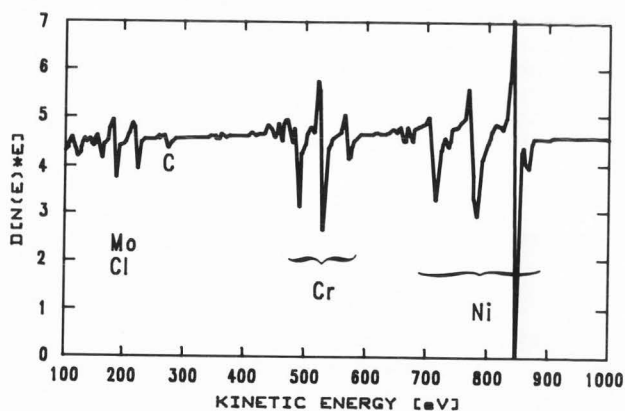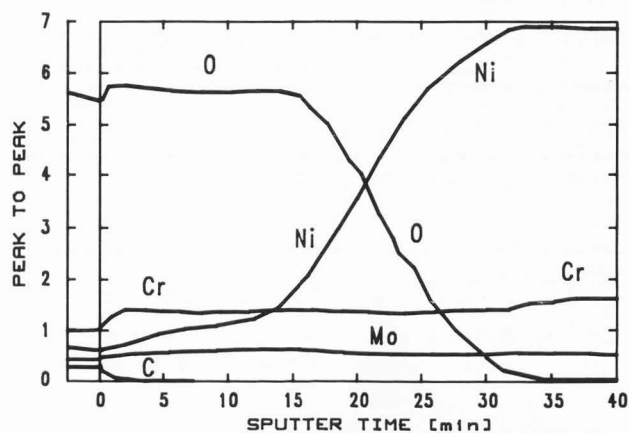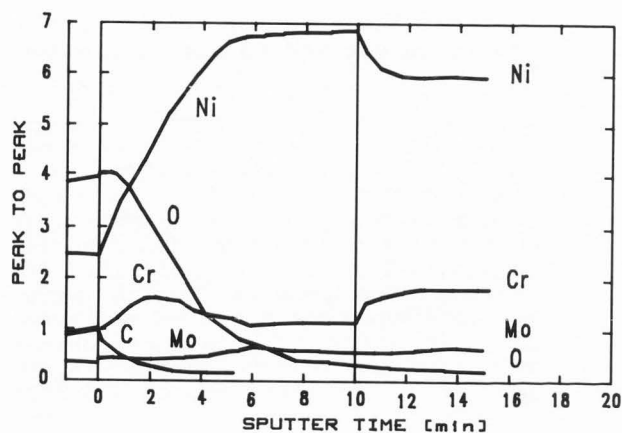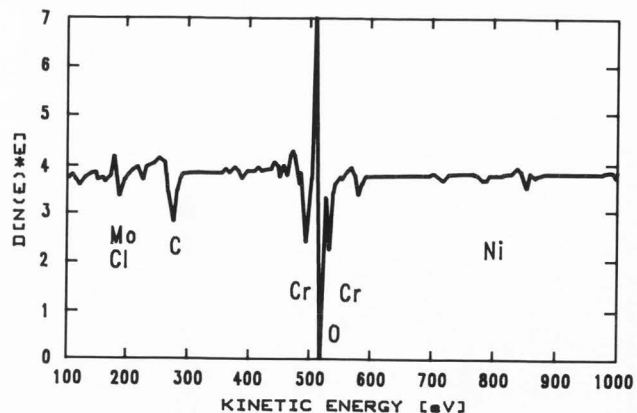
Fig. 11: AES spectrum of Ni-20Cr-10Mo polarized at 300 mV (SCE) in aerated 0.1 M NaCl for 20 h (before ion-milling).

Fig. 12: AES depth profile of Ni-20Cr- -10Mo, polarized at 300 mV (SCE) in aerated 0.1 M NaCl for 20 h (After 10 min. of sputtering the sputter rate was raised to a factor of 100).

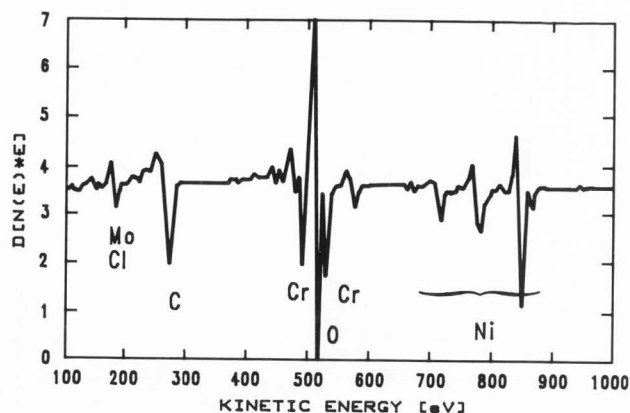**Fig. 13:** AES spectrum after registrating the depth profile of Fig. 12.

Fig. 14: AES spectrum of Ni-20Cr-10Mo, polarized at 650 mV (SCE) in aerated 0.1 M NaCl for 20 h (before ion-milling).

Fig. 15: AES depth profile of Ni-20Cr- -10Mo polarized at 650 mV (SCE) in aerated 0.1 M NaCl for 20 h.

Fig. 16: AES spectrum after registrating the depth profile of Fig. 15.

transpassive region (650 mV) was about 50 times thicker than that produced at 300 mV in the passive region.

Acknowledgment

References

[1] Baran G. (1984). Auger Chemical Analysis of Oxides on Ni-Cr Alloys. J Dent Res 63, 76-80

[2] Blanco-Dalmau L. (1982). The nickel problem. J Prosth Dent 48, 99-101

[3] Espevik S., Rapp A., Daniel P.L., Hirth, J.P. (1980). Oxidation of Ni-Cr-W Ternary alloys. Oxidation of Metals 14, 85-108

[4] Evans U.R. (1971). Inhibition, Passivity and Resistance: A review of acceptable mechanisms. Electrochimica Acta 16, 1825-1840

[5] Fisher A. (1973). Contact Dermatitis. 2nd ed., Philadelphia: Lea & Febiger, 745-761

[6] Geis-Gerstorfer J., Weber H. (1985). Effect of potassium thiocyanite on the corrosion behavior of dental base metal alloys. Dtsch Zahnärztl Z 40, 87-91

[7] Geis-Gerstorfer J., Sauer K.H., Weber H. (1986). In vitro corrosion bulk reduction in non-precious alloys. Dtsch Zahnärztl Z 41, 519-524

[8] Hoar T.P., Mears D.C., Rothwell G.P. (1965). The Relationships between Anodic Passivity, Brightning and Pitting. Corrosion Science 5, 279-289

[9] Kolotyrkin Ya.J. (1964). Pitting Corrosion of Metals. Corrosion 19, 261-268

[10] Sato N. (1971). A Theory for Breakdown of Anodic Oxide Films on Metals. Electrochimica Acta 16, 1683-1692

[11] Sato N., Kudo K., Noda T. (1971). The Anodic Oxide Film on Iron in neutral Solution. Electrochimica Acta 16, 1909-1921

[12] Strehblow H.H. (1984). Breakdown of passivity and localized corrosion: Theoretical concepts and fundamental experimental results. Werkstoffe und Korrosion 35, 437-448

Editor's Note: All of the reviewer's concerns were appropriately addressed by text changes, hence there is no Discussion with Reviewers.